Toward an Accurate and Efficient Theory of Physisorption. I. Development of an Augmented Density-Functional Theory Model

Garold Murdachaew*,†,‖

SISSA-ISAS: International School for Advanced Studies, Via Beirut 2-4, I-34014 Trieste, Italy

Stefano de Gironcoli‡

SISSA-ISAS and CNR-INFM DEMOCRITOS National Simulation Centre, Trieste, Italy

Giacinto Scoles§

SISSA-ISAS, CNR-INFM DEMOCRITOS, and Department of Chemistry, Princeton University, Princeton, New Jersey 08544

Received: February 1, 2008; Revised Manuscript Received: July 3, 2008

Currently available density functionals cannot describe the dispersion component of the interaction energy present in weakly bound complexes. Moreover, the exchange energy as obtained from the density-functional theory is often incorrect. Examples of problematic cases include clusters of van der Waals-bound rare-gas atoms and most hydrogen-bonded molecular systems. Thus, accurate ab initio methods to treat intermolecular forces should be used in such systems. These methods are, however, too slow to be applicable to the large systems needed to model adsorption. This is why DFT continues to be used, where, in addition, a quite common compensation of errors sometimes produces some sort of agreement with the corresponding experimental data. In this paper, we analyze in detail the inadequacy of standard DFT for describing the weak binding present in a few rare gas−rare gas, metal atom−rare gas, and metal atom−metal atom dimers. Inspired by the success of the Hartree−Fock plus (damped) dispersion (HFD) method, we test the use of an improved hybrid model in which to a density-functional interaction energy (with corrected exchange and avoidance of double-counting of dispersion), a (damped) dispersion expansion is added in the usual way. Comparisons with accurate theoretical or experimental benchmarks show that our DFdD method using the revPBEx or revPBEx+VWNc functionals and accurate dispersion coefficients is found to recover the interaction energy curves very well for many of the tested systems. The second paper in this series will describe the use of the DFdD method for physisorption for the previously well-studied (but not solved) case of Xe/Cu(111).

1. Introduction

Due to the technological importance of adsorbate−surface interactions,[1] in recent years much work has been carried out toward the goal of obtaining a first-principles understanding of such systems and their bonding mechanisms. Because of its computational agility, density-functional theory[2,3] (DFT) is widely used for modeling such extended systems. Recent successes include studies of dissociative adsorption and heterogeneous catalysis on transition-metal surfaces[4,5] and the modeling[6] of self-assembled monolayers of short thiols on a gold surface.

The above examples involve, however, chemisorption, a situation where the bonds between the adsorbate and substrate are localized and strong (1 to a few eV), with separation distances of about 2 Å or less. Moreover, if DFT in the generalized-gradient approximation is used, the substrate and underlying bulk metal are reasonably well-described (the errors in cohesion energies of transition metals are generally about 10% or less when PW91 and similar exchange-correlation functionals, such as PBE, are used.)[7] A correct theory of physisorption (for a recent monograph and reviews, see, e.g., refs 8, 9 and 10), on the other hand, is more challenging because it involves also adsorbate−surface interactions with larger adsorbate−surface separations and thus often the much weaker physical rather than chemical bonds (usually less than 0.5 eV per nonpolymeric molecular adsorbate). In contrast with chemisorption, for physisorbed systems no significant amount of charge is transferred or shared and the geometries and electronic structures of the isolated adsorbate and the substrate are not greatly changed but merely perturbed.

A simple and straightforward ab initio modeling approach is still lacking for physisorption because, in the case of weak or van der Waals bonding, accurate calculations with a careful treatment of the electron correlation are required in order to recover the dispersion component of the interaction energy. While DFT is in principle exact, the approximate DFT exchange-correlation (xc) functionals currently in use are of either local character or of semilocal character (generalized-gradient approximation or GGA, with an additional dependence or density gradients). These functionals, requiring charge overlap to result in an interaction, cannot recover the long-range correlation needed to represent the dispersion component that is present also at distances where charge overlap may be negligible.[11] Even the newer meta-GGA functionals (with

* To whom correspondence should be addressed.
† E-mail: garold.murdachaew@pnl.gov.
‡ E-mail: degironc@sissa.it.
§ E-mail: gscoles@princeton.edu.
‖ Present address: Chemical Sciences Division, Pacific Northwest National Laboratory, Richland, WA 99352.

10.1021/jp800974k CCC: $40.75
Published on Web 09/05/2008

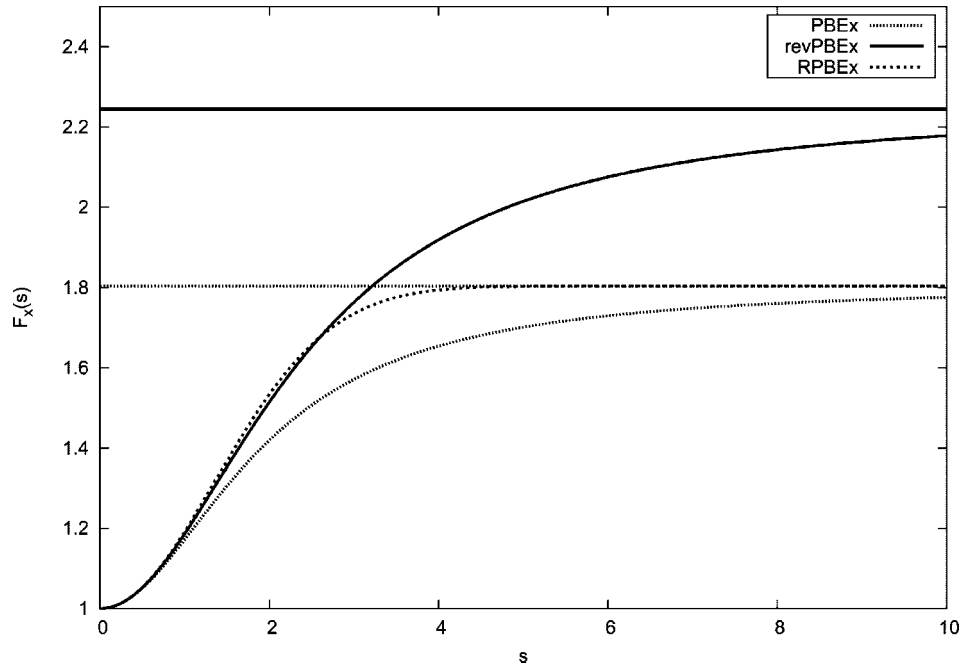

Figure 1. DFT exchange energy enhancement factor as a function of the reduced density gradient, for PBEx and its revised variants. Also shown are the large s limits $F_x^{PBEx}(s) = F_x^{RPBEx}(s) \rightarrow 1.804$ and $F_x^{revPBEx}(s) \rightarrow 2.245$.

TABLE 1: Basis Sets Used in the Calculations of Interaction Energies of the C_n Dispersion Coefficients[a]

center	basis set name (abbreviation)	ECP (valence, relativity)	refs	used to calculate
He	aug-cc-pVQZ (aQZ)	none	65	Mg−He: interactions (ae)
	aug-cc-pV5Z (a5Z)	none	65	Mg−He: C_n
Na	cc-pVTZ (TZ)	none	66	Na_2 and Na−Ar: DFT interactions
	aug-cc-pCVTZ (aCTZ)	none	66	Na_2 and Na−Ar: HF, MP2 (ae), and CCSD(T) (ae) interactions
Mg	aug-cc-pCVQZ (aCQZ)	none	66	Mg_2 and Mg−He: interactions (ae) and C_n
Ar	aug-cc-pVTZ (aTZ)	none	67	Ar_2 (fc), Na−Ar (DFT only), and Cu−Ar (fc) interactions
	aug-cc-pCVTZ (aCTZ)	none	67,68	Na−Ar: HF, MP2 (ae), and CCSD(T) (ae) interactions
Ca	aug′-cc-pCVTZ (aCTZ)[b,c,d]	none	38,69	Ca−Xe: interactions (ae)
	aug′-cc-pV5Z (a5Z)[b,c,e]	none	38,69	Ca−Xe: C_n
Cu	aug-cc-pVTZ-PP (aTZ-PP)	ECP10MDF (19, scalar)	57,60	Cu_2, Cu−Ar, and Cu−Xe: interactions (fc)
Kr	SDB-aug′-cc-pVTZ (SDB-aTZ)[b,f]	ECP28MWB (8, scalar)	56,58	Kr_2: interactions (fc)
Xe	SDB-aug′-cc-pVTZ (SDB-aTZ)[b,g]	ECP46MWB (8, scalar)	56,58	Xe_2 (fc), Ca−Xe (ae), and Cu−Xe (fc): interactions
	aug-cc-pV5Z-PP (a5Z-PP)	ECP28MDF (26, scalar)	59	Ca−Xe: C_n
midbond	33221[h]	none	20,54	H_2, He_2, Mg2 (ae), Mg−He (ae), and Ca−Xe (fc): interactions
	3322[i]	none	20,54	all other interactions

[a] Most basis sets/ECPs were downloaded from the web.[64] When the basis sets were used in MP2 or CCSD(T) calculations, the range of electrons included in the correlation treatment is indicated by the acronyms ae (all-electron; generally used for complexes with atoms requiring such treatment with the appropriate "CV"-type basis sets: Na, Mg, and Ca) or fc (frozen-core; used for complexes containing other atoms). Note that all C_n calculations were of ae type using the indicated basis sets. [b] The designation "aug′" indicates that the original basis set was supplemented by Gaussians with more diffuse exponents obtained using the even-tempered progression[70] of the original two most diffuse exponents in that symmetry. Since only a single function existed in the last symmetry of the original basis set, it was extended by assuming the same ratio as for the preceding symmetry. [c] This augmentation was done in ref 38 and was taken from this source. [d] The aug′ exponents are s: 0.0102 42; p: 0.0095 89; d:0.0122 53; f: 0.0444 03. [e] The aug′ exponents are s: 0.0088 90; p: 0.0089 68; d: 0.0100 94; f: 0.0286 67; g: 0.0338 78; h: 0.0848 30. [f] The aug′ exponents are s: 0.0511 202; p: 0.0333 619; d: 0.1266 01; f: 0.3011 15. [g] The aug′ exponents are s: 0.0491 626; p: 0.0287 357; d: 0.1186 57; f: 0.2675 91. [h] s and p: 0.9, 0.3, 0.1; d and f: 0.6, 0.2; g: 0.35. [i] s and p: 0.9, 0.3, 0.1; d and f: 0.6, 0.2.

additional dependence on the kinetic-energy density and/or the Laplacian of the density, e.g., TPSS[12]) are still only semilocal. Thus, standard DFT fails badly in the case of weak bonding,[13,14] and one must conclude that any good agreement with experiment or more accurate calculations for weakly bound systems is likely to be accidental. We note in passing that DFT-GGA, by its good description of the molecular electronic density and multipole moments, may perform reasonably well for weakly bonded systems such as water[13,14] in which the electrostatic interactions are dominant. Thus systems in which hydrogen-bonded structures dominate may be relatively well-represented by DFT xc functionals, such as PBE for example.[13–15]

It is by now well accepted that, in order to recover long-range correlations, a truly nonlocal DFT is necessary.[11] Indeed, some progress toward the goal of achieving a nonlocal DFT has been made by means of the adiabatic fluctuation−dissipation theorem (ACFDT; a route toward the random phase approximation or RPA). It is noteworthy that the recently described "EXX-RPA+" approach of Marini et al.[16] claims to address both the nonlocality and self-interaction error (SIE) problems simultaneously and claims good results for interlayer interactions in hexagonal boron nitride. This approach has not yet seen, however, broader application, and, as implemented thus far, this "exact" approach is still too expensive to be used routinely on

TABLE 2: Best Evaluated Values of the Ground-State Atomic First Ionization Potentials *I* (in eV) of the Studied Atoms

	I [a]
H	13.598
He	24.587
Na	5.139
Mg	7.646
Ar	15.759
Ca	6.113
Cu	7.726
Kr	14.000
Xe	12.130

[a] Reference 71.

extended systems. Finally, it is not clear if some of the simpler approximate implementations such as the vdW-DF approach[17–19] retain the necessary accuracy. For example, ref 20 showed that the interaction energy of Ar_2 and Kr_2 as given[17] by the vdW-DF approach is in substantial error compared to accurate calculations: for Ar_2 and Kr_2, the potential wells are too deep by 60% and 40%, respectively (and both are shifted outward by 5%). The substantial error in the well depths is comparable to those of DFT-GGA such as PBE (except that PBE generally makes the well depths too shallow by about the same amount).

As mentioned briefly above, an additional problem with the available xc functionals is the presence of a quite large self-interaction error (SIE) in the exchange functional, which can mimic the otherwise absent long-range correlation.[21] To some extent, this error may be canceled by the shortcomings of the correlation functional, but the results are unsatisfactory and highly system- and functional-dependent.

For these reasons, we adopt here the spirit of the successful Hartree−Fock plus (damped) dispersion (HFD) method (see refs 22 and 13 and additional references therein) and the similar density-functional plus (damped) dispersion (DFdD) method rigorously tested by Wu et al.[13] and would like to explore the possibility to develop a similar model (to be used later for extended systems) using DFT with long-range correlation added in the form of long-range damped dispersion energy (since dispersion coefficients are relatively easy and cheap to calculate precisely). We go further than ref 13 in that we aim and succeed at obtaining a good description between two rare gas atoms where the bonding is a factor of 10 weaker than in the systems successfully modeled in ref 13. Furthermore, we test additional GGA functionals like PBE (and various versions thereof), the hybrid PBE0, and the meta-GGA functional TPSS. To test the limits of our approach, we attempt to use accurate DFT and HF energies (and therefore larger basis sets than in ref 13) and accurate dispersion coefficients and damping. Like in ref 13, as much as possible, we attempt to avoid double-counting the long-range correlation, and thus we endeavor to employ only short-range, local correlation in the region where overlap is appreciable. Our final goal, after verifying the DFdD method on dimers, is to attempt to apply the recipe to an extended system, that of Xe/Cu(111) physisorption. This work is in progress and will be described in a second paper.

2. Calculational Details

2.1. General Remarks. As is well-known, van der Waals interactions are notorious for being the result of a very delicate balance between the different contributions of electrostatic, exchange, induction, and dispersion energies (to second order in intermolecular perturbation theory).[23,24] Since the interaction energies of such "molecules" are minuscule fractions of the total

TABLE 3: Dispersion Coefficients C_n (in Atomic Units, Hartree·bohr^n) and Damping Parameters ρ (in bohr^{-1}) of the Dimers Studied[a]

	C_6	C_8	C_{10}	C_{12}	C_{14}	ρ[q]
Rg_2 singlets						
Ar_2[b]	64.691[c]	1 644[d]	50 240[d]	1 898 195[e]	86 445 426[e]	1.103
Kr_2	129.48[c]	3 981[d]	147 400[d]	6 757 284[e]	373 923 452[e]	1.0194
Xe_2	282.72[c]	11 390[d]	562 117[f]	34 939 760[e]	2 666 668 208[e]	0.9273
M-Rg singlets						
Mg−He	21.77[g]	916[g]	47 214[f]	3 065 006[e]	244 315 090[e]	0.9351
Ca−Xe	604.23[h]	45 635[h]	4 222 114[f]	491 984 479[e]	70 392 931 290[e]	0.6635[r]
M-Rg doublets						
Na−Ar	188.7[i]	10 580[i]	726 667[f]	62 860 091[e]	6 676 835 151[e]	0.7123
Cu−Ar	128[m]	5 376[n]	276 595[f]	17 923 369[e]	1 426 102 741[e]	0.8476
Cu−Xe	267[k]	13 884[l]	884 411[f]	70 955 015[e]	6 989 857 458[e]	0.7903
M_2 singlet						
Mg_2	634.86[j]	43 578[j]	3 664 314[f]	388 067 935[e]	50 463 685 766[e]	0.6360[s]
M_2 triplets						
Na_2	1 556[o]	116 000[p]	11 300 000[p]	1 478 851 259[e]	253 491 076 845[e]	0.4945[t]

[a] Note that for C_n, $n \geq 10$, not all of the digits are significant. [b] Reference 28. [c] Reference 72. [d] Reference 73. [e] Extrapolated from C_6-C_{10} as prescribed by Thakkar.[74] [f] Extrapolated as $C_{10} = (49/40)C_8^2/C_6$.[74] [g] CKS value calculated with POLCOR[30,31] as described in ref 38; C_6 also given in ref 38. [h] CKS value calculated with POLCOR[30,31] as described in ref 38. [i] Reference 75. [j] CKS value calculated with POLCOR[30,31] as described in ref 38; C_6 also given in ref 38. [k] Obtained from the simple combination rule $C_6^{\text{Cu-Xe}} = (C_6^{\text{Cu}_2}C_6^{\text{Xe}_2})^{1/2}$ with $C_6^{\text{Cu}_2} = 253$ (value marked "Corrected" in Table XII of ref 76) and $C_6^{\text{Xe}_2}$ from above. [l] $C_8 = fC_6$, where $f = 52$ was obtained from rough optimization so as to bring the HFD values (including the effect of all damped dispersion coefficients) into reasonable agreement with the CCSD(T) values near the minimum of the potential curve. Note that a similar procedure was occasionally used in ref 13. [m] Obtained from the simple combination rule $C_6^{\text{Cu-Ar}} = (C_6^{\text{Cu}_2}C_6^{\text{Ar}_2})^{1/2}$ with $C_6^{\text{Cu}_2} = 253$ (value marked "Corrected" in Table XII of ref 76) and $C_6^{\text{Ar}_2}$ from above. [n] $C_8 = fC_6$, where $f = 42$ was obtained from rough optimization so as to bring the HFD values (including the effect of all damped dispersion coefficients) into reasonable agreement with the CCSD(T) values near the minimum of the potential curve. Note that a similar procedure was occasionally used in ref 13. [o] Reference 77. [p] Reference 78. [q] Calculated using eq 3 (or eq 4 for mixed complexes) from ionization potentials in Table 2. [r] Equation 4 yielded 0.7212; however, this was not sufficient damping and thus this value was scaled by a factor of 0.92 (obtained from rough optimization). [s] Equation 4 yielded 0.6839; however, this was not sufficient damping and thus this value was scaled by a factor of 0.93 (obtained from rough optimization). [t] Equation 4 yielded 0.5261; however, this was not sufficient damping and thus this value was scaled by a factor of 0.94 (obtained from rough optimization).

TABLE 4: Deviations from the HF Values of the DFT Interaction Energies (in Percent) and of the DFT Total Energies (in Hartree) of Some Representative Complexes at the Near-Minimum CCSD(T) or Literature Geometries[a]

	Rg_2						M-Rg						M_2					
	(R = 3.75 Å)			(R = 4.42 Å)			(R = 5.1 Å)			(R = 3.9 Å)			(R = 3.9 Å)			(R = 5.2 Å)		
Method	Ar_2 int [cm^{-1}]	Ar_2 tot [Hartree]	Ar tot [Hartree]	Xe_2 int [cm^{-1}]	Xe_2 tot [Hartree]	Xe tot [Hartree]	Ca−Xe int [cm^{-1}]	Ca−Xe tot [Hartree]	Ca tot [Hartree]	Cu−Xe int [cm^{-1}]	Cu−Xe tot [Hartree]	Cu tot [Hartree]	Mg_2 int [cm^{-1}]	Mg_2 tot [Hartree]	Mg tot [Hartree]	Na_2 int [cm^{-1}]	Na_2 tot [Hartree]	Na tot [Hartree]
LDAx	−242%	4.62	2.31	−217%	0.38	0.19				−203%	0.79	0.60				−357%	2.45	1.22
LDA	−290%	1.76	0.88	−262%	−0.39	−0.20	−235%	0.82	1.02	−241%	−0.98	−0.78	−333%	0.96	0.48	−384%	0.84	0.42
PBEx	**−33%**	**0.36**	**0.18**	**−12%**	**−0.03**	**−0.01**				−62%	**−0.27**	**−0.25**				−78%	**0.12**	**0.06**
PBEx+VWNc	−111%	−2.50	−1.25	−81%	−0.80	−0.40				−112%	−2.04	−1.64				−123%	−1.49	−0.74
PBE	−133%	−1.05	−0.52	−120%	−0.52	−0.26	−150%	−0.85	−0.59	−141%	−1.40	−1.13	−259%	−0.76	−0.37	−203%	−0.69	−0.34
revPBEx	113%	**0.14**	**0.07**	98%	**−0.08**	**−0.04**	**11%**	**0.03**	**0.07**	**2%**	**−0.34**	**−0.30**	**−14%**	**−0.01**	**−0.01**	**0.3%**	**−0.03**	**−0.01**
revPBEx+VWNc	**20%**	−2.72	−1.36	**20%**	−0.85	−0.43	−47%	−1.94	−1.52	−51%	−2.12	−1.69	−85%	−1.80	−0.90	−48%	−1.64	−0.82
revPBE	**−4%**	−1.27	−0.64	**−17%**	−0.57	−0.29	−78%	−0.99	−0.71	−77%	−1.47	−1.18						
RPBEx	**22%**	**0.06**	**0.03**	48%	**−0.08**	**−0.04**				**−16%**	**−0.36**	**−0.32**				**−6%**	**−0.08**	**−0.04**
RPBEx+VWNc	−69%	−2.80	−1.40	**−31%**	−0.86	−0.43				−69%	−2.14	−1.70				−56%	−1.69	−0.84
RPBE	−92%	−1.35	−0.68	−68%	−0.58	−0.29				−95%	−1.49	−1.20				−140%	−0.82	−0.41
PBE0	−116%	−1.27	−0.63	−111%	−0.53	−0.26	−132%	−0.97	−0.70	−118%	−1.36	−1.09	−234%	−0.79	−0.39	−175%	−0.72	−0.36
TPSSx	**21%**	**−0.08**	**−0.04**	**34%**	**−0.03**	**−0.02**				**−34%**	**−0.20**	**−0.18**				−246%	−0.87	−0.44
TPSSx+VWNc	−59%	−2.94	−1.47	−36%	−0.81	−0.40				−83%	−1.97	−1.57				−69%	**−0.13**	**−0.06**
TPSS	−73%	−1.49	−0.75	−66%	−0.53	−0.27				−108%	−1.33	−1.06				−117%	−1.74	−0.87
HF	96	−1053.63	−526.81	172	−30.55	−15.28	223	−692.03	−676.76	480	−211.45	−196.18	581	−399.23	−199.61	145	−323.72	−161.86

[a] The percentage deviations that are less than 35% (in absolute value) are shown in bold font, as are the smallest deviations (in absolute value) of the total energies. The HF values are shown at the bottom of the table. The standard basis sets from Table 1 were used.

energies of the complex and its component parts, if the interaction energy is to be obtained by subtraction (as is done in all so-called supermolecular approaches), the errors in each of the total energies of the complex and its components have to be smaller or fortuitously cancel. Such a cancelation apparently does take place for the HF method (which, however, lacks the important dispersion interactions) and the properly used post-HF methods, see below. It must be noted that, when studying weak interactions with a supermolecular approach and using localized and finite basis sets, it is crucial to apply the counterpoise (CP) correction[25] to avoid the basis set superposition error (BSSE).

The study of weak interactions requires a post-HF treatment in order to recover the correlation energy and therefore the often critical dispersion interaction. Thus, with a supermolecular approach,[26] the correct description of weakly bound systems requires use of at least MP2 (Möller-Plesset method of second order), or, much better, CCSD(T) (coupled-cluster expansion including single, double, and (noniterated) triple excitations,[27]) the most accurate of readily available and affordable supermolecular methods, at least for small- and medium-size systems comprising less than 20 atoms in the dimer. For recent examples, see, e.g., refs 28 and 29.

It should be mentioned that another extremely robust approach for studying weakly bound systems containing van der Waals or hydrogen bonds is the symmetry-adapted perturbation theory[23,24] (SAPT) of intermolecular interactions. First, unlike the supermolecular methods, it does not require subtraction and thus is inherently free of BSSE and therefore allows a more flexible use of basis sets. More importantly, it yields detailed information on the interaction in the form of its decomposition into its physically interpretable components: in first order of SAPT, the electrostatic and exchange energies, and, in second order, the induction and dispersion energies and their exchange counterparts, the exchange-induction and exchange-dispersion energies. Since the exchange components (and the overlap portions of all components) decay exponentially with intermolecular separation, at long-range the remaining components obtained from SAPT, the electrostatic energy (present if both monomers have permanent multiple moments), the induction energy (present if at least one monomer has such moments), and the dispersion energy (always present), can be compared to their asymptotic values, which are easily interpretable in terms of asymptotic coefficients formed from proper combinations of the monomers' properties (multipole moments and static and dynamic polarizabilities). Since packages such as POLCOR[30,31] can calculate monomer properties and asymptotic coefficients of closed-shell complexes, there exists a direct check on the SAPT interaction energy components at long-range. Recently, SAPT(DFT),[32–36] a version of SAPT that uses a DFT description of monomers (since DFT can be quite accurate for the strong, short-range chemical intramonomer interactions and has the advantage over HF in that the short-range correlation is already included) has been successfully developed. By eliminating the need for calculating intramonomer correlation corrections, the new method is many times faster than SAPT. For recent examples of the use of SAPT and SAPT(DFT), see, e.g., refs 20, 37, and 38.

With continuing advances in software[39] and hardware, the size of systems treatable with high accuracy will slowly grow. However, it is still difficult or impossible to perform today CCSD(T) or SAPT(DFT) calculations, with sufficiently large basis sets for true accuracy, for systems with a few tens to one hundred atoms. This is because using the accurate approaches

TABLE 5: Values of the Characteristic Features of Each Complex As Obtained with Different Methods: (a) Bond Length R_e; (b) Binding Energy $D_e = -E_{int,min}$; and (c) Harmonic Frequency ω_e[a]

(a) R_e [Å] and % ΔR_e (in parentheses); and rmsd [Å]

	Rg_2				M-Rg						M_2		
method	Ar_2	Kr_2	Xe_2	rmsd	Mg−He	Ca−Xe	Na−Ar	Cu−Ar	Cu−Xe	rmsd	Mg_2[p]	Na_2	rmsd
DFT													
LDA	3.42 (−10%)			0.40					2.66 (−32%)	1.25			
PBE	4.04 (6%)			0.22					3.10 (−21%)	0.81			
revPBE	4.65 (22%)			0.83					5.62 (44%)	1.71			
RPBE	4.24 (11%)			0.42					4.82 (23%)	0.91			
PBE0	4.08 (7%)			0.26					3.94 (1%)	0.03			
TPSS	4.31 (13%)			0.49					3.62 (−7%)	0.29			
DFdD													
LDAx + dD	3.25 (−15%)			0.57					2.58 (−34%)	1.33			
LDAx ext + dD	3.13 (−18%)			0.69					2.93 (−25%)	0.98			
PBEx + dD	3.86 (1%)			0.04					3.11 (−20%)	0.79			
PBEx ext + dD	3.83 (0%)			0.01					3.71 (−5%)	0.20			
revPBEx + dD	4.31 (13%)	4.61 (13%)	4.97 (11%)	0.51	4.86 (−6%)	5.48 (7%)	4.97 (−3%)	4.29 (4%)	3.68 (−6%)	0.24	3.75 (−4%)	4.70 (−9%)	0.36
revPBEx ext + dD	4.17 (9%)	4.51 (11%)	4.82 (8%)	0.39	5.06 (−2%)	5.03 (−2%)	4.62 (−9%)	4.07 (−1%)	3.79 (−3%)	0.23	3.94 (1%)	5.11 (−2%)	0.06
revPBEx+VWNc + dD	4.01 (5%)	4.26 (5%)	4.58 (3%)	0.17	4.44 (−14%)	4.77 (−7%)	4.04 (−21%)	3.73 (−9%)	3.24 (−17%)	0.69	3.37 (−14%)	4.49 (−13%)	0.62
revPBEx+VWNc ext + dD	3.92 (3%)	4.10 (1%)	4.50 (1%)	0.07	4.07 (−21%)	4.42 (−14%)	3.80 (−25%)	3.49 (−15%)	3.61 (−8%)	0.87	3.48 (−11%)	4.69 (−10%)	0.46
RPBEx + dD	4.07 (7%)			0.25					3.74 (−4%)	0.16			
RPBEx ext + dD	3.92 (3%)			0.10					3.87 (−1%)	0.03			
TPSSx + dD	4.03 (6%)			0.21					3.19 (−18%)	0.71			
TPSSx ext + dD	3.91 (2%)			0.09					3.55 (−9%)	0.36			
HFD	3.76 (−2%)	4.02 (−1%)	4.36 (−2%)	0.07	5.29 (3%)	5.13 (0%)	5.06 (−1%)	4.10 (0%)	3.84 (−2%)	0.07	4.08 (5%)	5.19 (0%)	0.15
MP2	3.77 (−1%)	4.02 (−1%)	4.38 (−2%)	0.06	5.21 (1%)	4.99 (−3%)	5.24 (3%)	4.07 (−1%)	3.95 (1%)	0.10	4.00 (3%)	5.88 (13%)	0.07
CCSD(T) benchmark	3.82	4.07	4.46		5.15	5.14	5.09	4.12	3.91		3.98	5.19	
literature benchmarks													
ab initio 1	3.767[b]	4.037[d]	4.420[d]		5.0[g]	5.17[i]		4.00[k]			3.9[l]	5.192[n]	
ab initio 2					5.1[h]								
empirical	3.757[c]	4.011[e]	4.366[f]				4.994[j]				3.9[m]		

(b) D_e [cm^{-1}] and % ΔD_e (in parentheses); and rmsd [cm^{-1}]

	Rg_2				M−Rg						M_2		
method	Ar_2	Kr_2	Xe_2	rmsd	Mg−He	Ca−Xe	Na−Ar	Cu−Ar	Cu−Xe	rmsd	Mg_2[p]	Na_2	rmsd
DFT													
LDA	244 (152%)			147					2628 (1163%)	2420			
PBE	48 (−51%)			49					346 (66%)	138			
revPBE	14 (−86%)			83					13 (−94%)	195			
RPBE	52 (−46%)			45					56 (−73%)	152			
PBE0	31 (−68%)			66					88 (−58%)	120			
TPSS	28 (−71%)			69					41 (−80%)	167			
DFdD													
LDAx + dD	552 (468%)			455					4869 (2239%)	4661			
LDAx ext + dD	417 (329%)			320					547 (163%)	339			
PBEx + dD	138 (43%)			41					875 (320%)	667			
PBEx ext + dD	144 (48%)			47					613 (194%)	404			
revPBEx + dD	62 (−36%)	75 (−44%)	98 (−45%)	61	20 (328%)	114 (−18%)	57 (50%)	92 (14%)	243 (17%)	23	476 (7%)	200 (12%)	26
revPBEx ext + dD	53 (−46%)	58 (−56%)	95 (−47%)	70	5 (−4%)	113 (−19%)	36 (−4%)	78 (−3%)	247 (18%)	21	468 (5%)	179 (0%)	16
revPBEx+VWNc + dD	102 (5%)	128 (−4%)	175 (−2%)	5	38 (697%)	250 (80%)	205 (444%)	218 (169%)	694 (234%)	243	1060 (138%)	322 (80%)	446
revPBEx+VWNc ext + dD	100 (3%)	123 (−8%)	199 (11%)	13	23 (390%)	344 (147%)	192 (409%)	264 (225%)	569 (173%)	214	1021 (129%)	275 (54%)	413
RPBEx + dD	121 (24%)			23					324 (56%)	116			
RPBEx ext + dD	112 (15%)			14					340 (63%)	132			
TPSSx + dD	103 (6%)			5					595 (186%)	387			

TABLE 5 (Continued)

(b) D_e [cm^{-1}] and % ΔD_e (in parentheses); and rmsd [cm^{-1}]

	Rg_2				M−Rg						M_2		
method	Ar_2	Kr_2	Xe_2	rmsd	Mg−He	Ca−Xe	Na−Ar	Cu−Ar	Cu−Xe	rmsd	Mg_2[p]	Na_2	rmsd
TPSSx ext + dD	96 (−1%)			1					484 (132%)	276			
HFD	104 (7%)	143 (8%)	207 (16%)	18	4 (−18%)	130 (−7%)	32 (−16%)	77 (−5%)	243 (17%)	17	392 (−12%)	167 (−6%)	38
MP2	109 (12%)	158 (19%)	226 (27%)	32	4 (−7%)	203 (46%)	30 (−19%)	106 (30%)	246 (18%)	35	411 (−8%)	53 (−70%)	92
CCSD(T) benchmark	97	133	178		5	139	38	81	208		365	178	
literature benchmarks													
ab initio 1	99.27[b]	135.09[d]	183.08[d]		5.10[g]	131.4[i]		89.3[k]			445[l]	177.7[n]	
ab initio 2					5.00[h]								
Empirical	99.55[c]	139.91[e]	196.56[f]				40.4[j]				431[m]		

(c) ω_e [cm^{-1}] and % $\Delta\omega_e$ (in parentheses); and rmsd [cm^{-1}]

	Rg_2				M-Rg						M_2		
method	Ar_2	Kr_2	Xe_2	rmsd	Mg−He	Ca−Xe	Na−Ar	Cu−Ar	Cu−Xe	rmsd	Mg_2[p]	Na_2	rmsd
DFT													
LDA	66 (113%)			35					130 (584%)	111			
PBE	24 (−23%)			7					35 (84%)	16			
revPBE	12 (−61%)			19					4.3 (−77%)	15			
RPBE	23 (−26%)			8					9.3 (−51%)	10			
PBE0	17 (−45%)			14					14 (−26%)	5			
TPSS	16 (−48%)			15					6.4 (−66%)	13			
DFdD													
LDAx + dD	87 (179%)			56					134 (618%)	115			
LDAx ext + dD	92 (195%)			61					40 (116%)	22			
PBEx + dD	29 (−8%)			3					49 (161%)	30			
PBEx ext + dD	65 (107%)			33					51 (176%)	33			
revPBEx + dD	18 (−41%)	14 (−42%)	11 (−42%)	11	18 (67%)	12 (−37%)	12 (7%)	14 (−13%)	18 (−2%)	5	74 (53%)	33 (29%)	19
revPBEx ext + dD	26 (−15%)	13 (−44%)	14 (−31%)	7	10 (−6%)	17 (−8%)	13 (15%)	17 (2%)	24 (31%)	3	56 (15%)	26 (0%)	5
revPBEx+VWNc + dD	27 (−15%)	17 (−28%-)	15 (−23%)	5	27 (149%)	17 (−5%)	27 (132%)	21 (24%)	42 (128%)	15	62 (29%)	45 (74%)	17
revPBEx+VWNc ext + dD	40 (28%)	22 (−6%)	23 (19%)	6	30 (182%)	32 (75%)	35 (196%)	37 (122%)	43 (129%)	20	86 (77%)	32 (24%)	27
RPBEx + dD	32 (4%)			1					22 (18%)	3			
RPBEx ext + dD	47 (51%)			16					30 (59%)	11			
TPSSx + dD	27 (−14%)			4					43 (130%)	24			
TPSSx ext + dD	37 (19%)			6					40 (113%)	21			
HFD	32 (3%)	24 (3%)	24 (20%)	2	12 (13%)	17 (−7%)	10 (−16%)	15 (−9%)	22 (21%)	2	57 (18%)	24 (−7%)	1
MP2	33 (7%)	25 (6%)	23 (15%)	2	12 (8%)	19 (4%)	12 (3%)	18 (8%)	22 (17%)	2	53 (10%)	17 (−35%)	1
CCSD(T) benchmark	31	24	20		11	18	12	17	19		48	26	
literature benchmarks													
ab initio 1[o]	31	24	20									26	
ab initio 2[o]													
empirical[o]	31	24	21				13						

[a] The names of the best-performing DFdD methods are in bold and their results can be compared to the HFD, MP2, and benchmark reults. In each sub-table, also shown for each method is the root mean square deviation relative to the CCSD(T) value (relative to the literature FCI value for Mg_2, R_e and D_e only, see footnote *k*), given separately for the three Rg_2, the five M-Rg, and the two M_2 complexes. The CCSD(T) values (and literature benchmarks if available) are shown at the bottom of each sub-table. Details of the DFdD method with extrapolation of the DFTx points are given as follows: For each complex, the DFdD method with extrapolation of the DFTx points used a fitting region [R_1, R_2] (in Å) as follows: Ar_2: [3.75,3.90] but [2.50,3.00] was used with LDAx; Kr_2: [2.50,4.30]; Xe_2: [4.00,5.00]; Mg−He: [2.50,4.00]; Ca−Xe: [2.50,5.50]; Na−Ar: [3.00,3.50]; Cu−Ar: [2.00,4.00]; Cu−Xe: [3.50,4.50]; Mg_2: [3.00,4.00]; and Na_2: [2.00,5.50]. [b] Ab initio potential: CCSD(T)/CBS + Δ (core-valence effects), ref 28. [c] Empirical potential: HFDID1, ref 79. [d] Ab initio potential: CCSD(T)/scalar relativistic ECPs with large basis set, ref 80. [e] Empirical potential: HFD-B2, ref 81. [f] Empirical potential: HFD-B2, ref 82. [g] Ab initio potential: CCSD(T)/CBS + Δ (FCI) + Δ (core-valence effects), ref 38. [h] Ab initio potential: CCSD(T)/CBS + Δ (full-triples) + Δ (core-valence effects), ref 83. [i] Ab initio potential: CCSD(T)/scalar relativistic ECPs with large basis set + Δ (core-valence effects/CPP), ref 84. [j] Empirical potential, ref 85. [k] Ab initio potential: CCSD(T)/scalar relativistic ECPs with large basis set, ref 86. [l] Ab initio potential (nonrelativistic estimate): CCSD(T)/CBS + Δ(FCI) + Δ(core-valence effects), ref 38. [m] Empirical potential: reanalyzed experimental estimate, ref 87. [n] Ab initio potential: CCSD(T)/large basis set with core-valence effects included, ref 88. [o] Values obtained by us with harmonic approximation using the appropriate potential cited in subtables 5(a-b) (for cases where full potential curves were available). [p] The benchmark here is the FCI value and differences are given relative to this value; see footnote *l*.

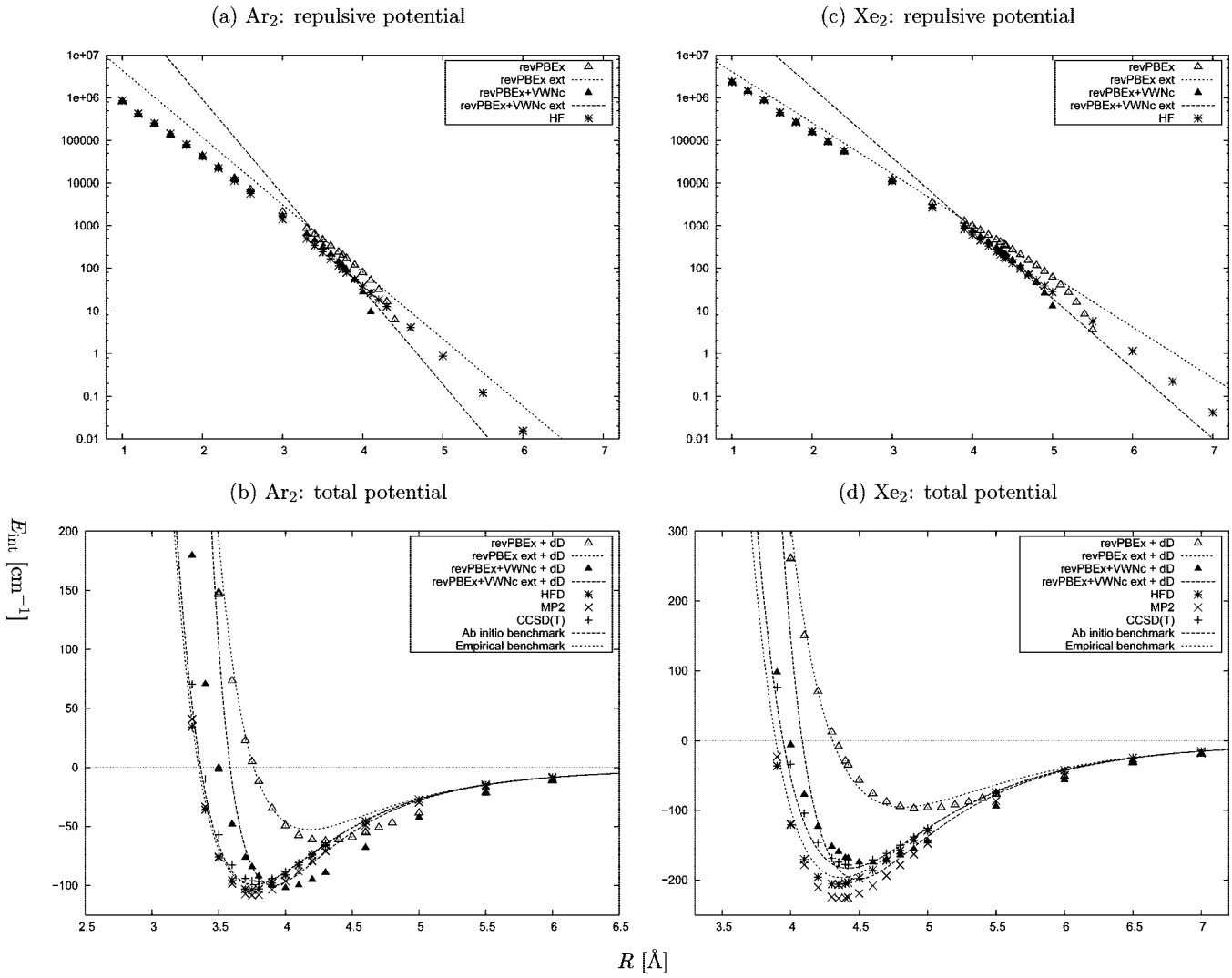

Figure 2. Interaction energies of the Rg_2 complexes Ar_2 and Xe_2. (The references for the benchmarks are given in Table 5.)

mentioned above for extended systems is hindered by their prohibitive scaling with system size, N (where N can be taken to be number of atoms, or valence/explicitly treated electrons). While DFT (with LDA or GGA nonhybrid xc functionals) and HF scale as N^4 (in practice DFT scales as N^3 in many plane-wave pseudopotential packages and HF and DFT scale similarly if density fitting is used in atomic codes with localized basis sets), the post-HF methods scale as N^5 (MP2), N^6 [MP4, CCSD, or SAPT(DFT)], and N^7 [SAPT or CCSD(T)]. Note that, with density fitting, the scaling has recently been reduced[40] to N^5 for SAPT(DFT), allowing single-processor calculations on an RDX dimer, with 42 atoms in the dimer. However, for truly metallic systems, there is an additional problem, which is the difficulty, or impossibility, of localizing the electronic wave functions, a necessity of the treatments mentioned above.

2.2. Levels of Theory. In this work, to prepare for calculations on extended systems and test our DFdD method, we have performed density-functional[2,3] calculations of the interaction energy produced by charge overlap. The exchange-correlation (xc) functionals used were the local xc functional LDA (Slater[41] exchange with VWN,[42] correlation) and the GGA xc functionals PBE,[43] revPBE,[44] and RPBE.[45] The hybrid functional PBE0[46] and the meta-GGA xc functional TPSS[12] were also tested. We also considered the effect of the exchange functional alone, or sometimes in combination with local correlation. Thus, for example, the meaning of the labels revPBEx and revPBEx+VWNc should be clear.

The only difference between the functionals PBE, revPBE, and RPBE is in the exchange portion, where they differ in the enhancement factor $F_x(s)$. Here $s = |\nabla n|/(2(3\pi^2)^{1/3}n^{4/3})$ is the reduced density gradient, and $n(\mathbf{r})$ is the electron density. The exchange energy itself is a functional of the density and is given by

$$E_x[n] = \int \mathrm{d}r\, n\varepsilon_x^{\mathrm{unif}} F_x(s) \tag{1}$$

where

$$\varepsilon_x^{\mathrm{unif}}(r) = -\frac{3}{4}\left(\frac{3}{\pi}\right)^{1/3} n(r)^{1/3} \tag{2}$$

is the local density per particle for a uniform electron gas and thus $F_x^{\mathrm{LDAx}}(s) = 1$ by definition. Figure 1 shows $F_x(s)$ for these exchange functionals. It is seen that the major differences are at larger values of s, where in fact, DFT is poorly defined/constrained. Indeed, this freedom has already been exploited in improving the performance of GGA xc functionals on weakly interacting systems, and for example, refs 44 and 45 presented revised versions of the exchange part of the PBE functional with improved performance. It is tempting to conclude that a good performance of one of these exchange functionals over

the others is due to its behavior at larger s values, and, in fact Zhang et al.[47] and Lacks et al.[48] have performed work that supports this view, and this work was already noted in ref 13. However, based on our results, it seems that there is still room for improvement in the larger s region of GGA exchange functionals, and if done systematically, this would be a useful contribution. It should be noted that such an improvement in the large s behavior should have no adverse effects on the good performance of GGA for more strongly interacting systems, since they depend only on the small s (and correspondingly large n) behavior, which would remain unchanged.

We also examined the HF (purely repulsive for the dimers considered here) and also the MP2 and CCSD(T) interaction energies. HF served as our benchmark for the exchange part of the interaction energy while the CCSD(T) value was the benchmark for the total interaction energy. (Note that Mg_2 requires a higher level of correlation, and thus the benchmark[38] for this system was the full configuration interaction−or FCI−correction to CCSD(T).) We also compared to literature benchmarks where they were available. Such a comparison confirmed that the basis sets used and the CCSD(T) method gave quite good results.

Most of the calculations on dimers were performed using the MOLPRO package.[49] However, for all dimers considered, the RPBE calculations were performed using the NWCHEM package,[50] while the TPSS calculations were performed with the NWCHEM package[50] for Ar_2, and the GAUSSIAN package[51] for Xe_2 and Cu−Xe. In all atomic packages a few test calculations were performed to ensure that convergence was achieved and convergence settings were comparable and that essentially the same interaction energy was recovered with the various packages.

For open-shell species, we used the restricted open-shell HF or DFT approach (RHF or RKS). Post-HF correlation treatment was also of the restricted variety (e.g., RMP2 and RCCSD(T), as described in refs 52 and 53 and implemented in the MOLPRO program package.)[49] However, for simplicity we will use the labels HF, MP2, CCSD(T), etc. and the "R" prefix will be taken to be understood as appropriate.

2.3. Basis Sets. Since adequate basis sets are very important for van der Waals complexes, we used basis sets of at least triple-ζ (TZ) quality, with diffuse functions, such as the Dunning group aug-cc-pVTZ (aTZ) sets (which can be considered to be of only medium quality for post-HF, correlated calculations such as MP2 or CCSD(T) but should be sufficient for HF and DFT calculations, the main topic of our study). For dimers with small atoms (or for calculations of dispersion coefficients), larger basis sets were affordable. The counterpoise[25] (CP) correction was used in all supermolecular calculations to avoid the basis set superposition error (BSSE). The details of the basis sets used are given in Table 1.

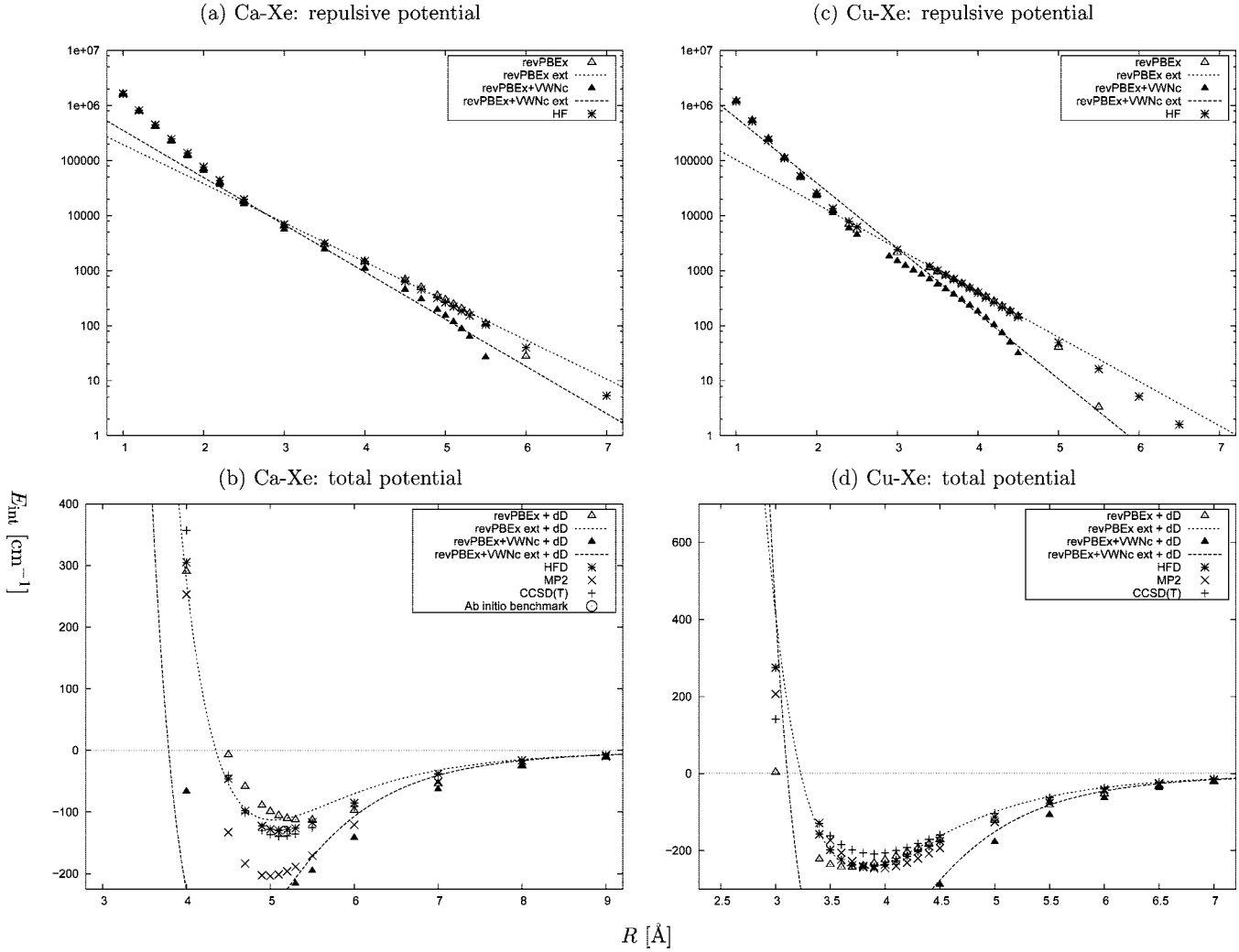

Figure 3. Interaction energies of the M-Rg complexes Ca−Xe and Cu−Xe (doublet). (The references for the benchmarks are given in Table 5.)

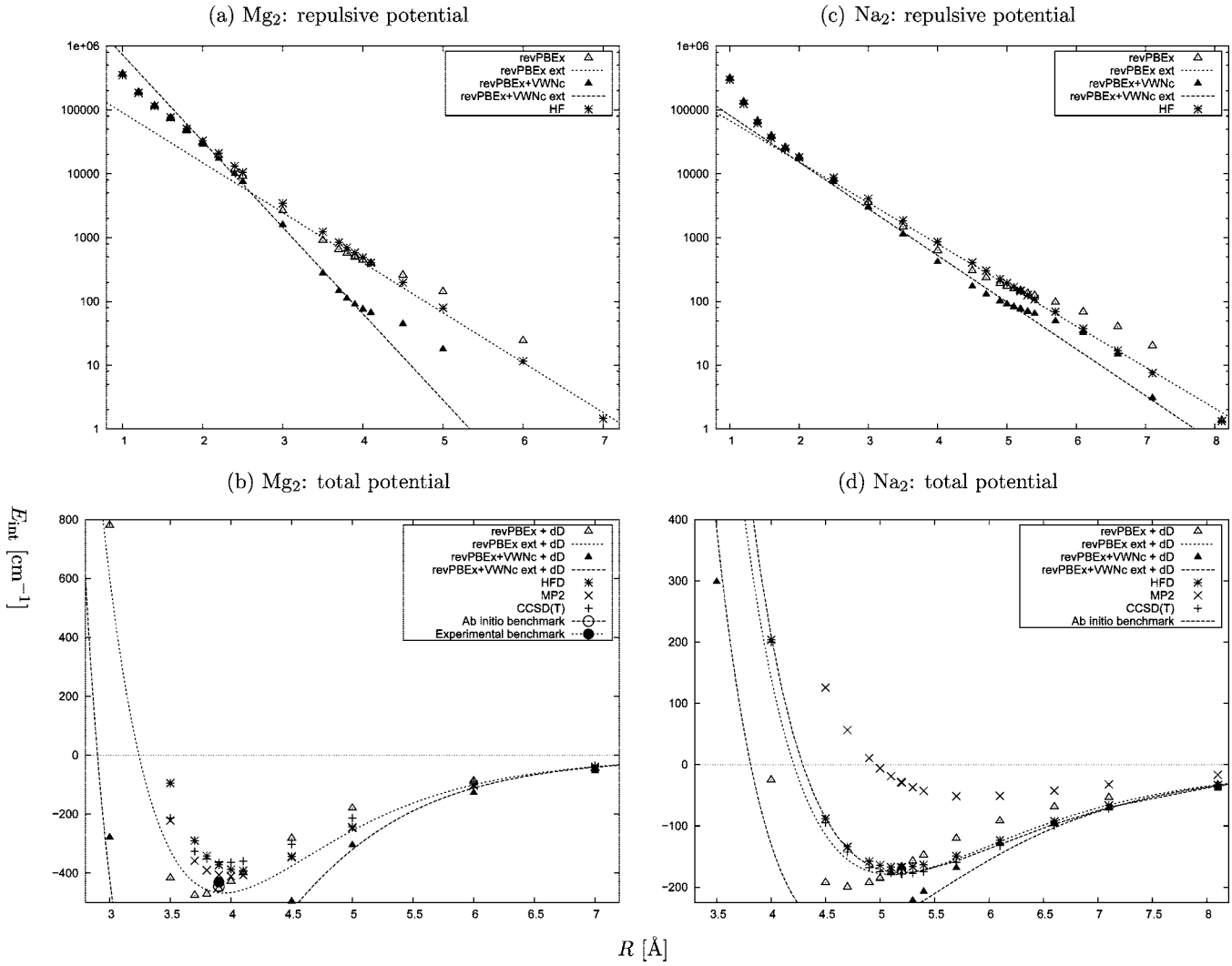

Figure 4. Interaction energies of the M_2 complexes Mg_2 and Na_2 (triplet). (The references for the benchmarks are given in Table 5.)

Having a balanced atomic basis set including diffuse functions is of primary importance. Thus, for Kr, Xe, and Ca, we augmented the exponents of the Gaussian atomic basis sets by an even-tempered extension of the two most diffuse functions in each symmetry (it is well-known that basis sets with such "aug" diffuse exponents are better able to describe polarizabilities, electron affinities, and thus dispersion interaction and the weak van der Waals bonding).

A set of bond functions was placed at the midpoint of the dimer. Such midbond functions are known to be effective in accelerating the convergence of the dispersion component of the interaction energy and in general, to efficiently approximate results obtained with purely atomic basis sets of much larger sizes (with more diffuse functions) and are thus particularly useful in the study of weak interactions.[20,54,55] For certain complexes (e.g., Ar_2, Xe_2, and Cu−Xe), to confirm that our basis sets were sufficiently large, we also performed some test calculations using smaller and larger basis sets, both with and without the bond functions. In all cases, we found that the bond functions improved the convergence of the interaction energies.

For the heavier atoms (Kr, Xe, and Cu), in order to include the scalar relativistic effects and to reduce the cost of calculations (and also to allow a better comparison with our calculations on surfaces to be described in the subsequent paper), we used quasi-relativistic Wood-Boring type effective core potentials (ECPs) of the Stuttgart-Dresden-Bonn group.[56,57] For the most part, we attempted to use small-core ECPs. However, in the case of Xe, we found that using a large-core ECP[56] and the accompanying basis set[58] (augmented by us, see Table 1 for details) had an insignificant effect on the interaction energies as compared to using the newer, somewhat more accurate (but more expensive) small-core ECP and accompanying valence basis set.[59] The CCSD(T) (frozen core, see below) test calculations were done on Xe_2, always together with the 3322 midbond functions. The ECP/basis set used for Kr was analogous to that used for Xe. For Cu, the Peterson et al.[60] basis set was used with the Figgen et al.[57] relativistic small-core ECP. Our choices are in agreement with the recommendations given in ref 61 for performing accurate ab initio calculations on weakly bound complexes with ECPs.

Most correlated calculations were performed in frozen core (fc) mode (i.e., only valence electrons participated in the correlation treatment) rather than in all-electron (ae) mode. The exceptions to this were the calculations for Mg_2, Mg−He, Na_2, Na−Ar, and Ca−Xe, all dimers containing atoms where core-valence effects are obviously important. Basis sets containing tighter exponents to model such effects were used in these cases.

For some of the dimers, we compared our CCSD(T) potentials to accurate literature ab initio potentials and also to accurate empirical potentials, if available. In all cases, we found that the agreement of our CCSD(T) results with the literature results was very good, while not being overly demanding of computer

time. This served as a check that aTZ-quality basis sets (plus midbond functions) are sufficient and that the various approximations we made (fc calculations for the correlation energy for many of the complexes) did not adversely affect the results. Since DFT and HF calculations converge much faster with basis set size (and are virtually unaffected by the presence or absence of augmentation functions or midbond functions, for basis sets of TZ-quality and higher that we used), our HF and DFT interaction energies can be considered to be well-converged with regard to basis set size.

2.4. HFD and DFdD Methods. In the HFD method one relies on the HF interaction energy to supply the repulsive (or exchange) part of the interaction of van der Waals complexes. Then the missing attraction (long-range correlation or dispersion) part is modeled by a dispersion energy expansion with dispersion coefficients C_n. The DFdD method simply replaces the HF by a DFT interaction energy, computed with an exchange-only or an exchange-local correlation only functional, to avoid double-counting of the long-range correlation to be correctly supplied by the dispersion expansion.

The HFD or DFdD methods require damping of the dispersion energy expansion. We used the universal damping formula introduced by Douketis et al.[22] with damping parameter, for a homonuclear dimer AA

$$\rho_{AA} = (I_A/I_H)^{0.66} \tag{3}$$

where the ionization potentials I_A and I_H are those of species A and hydrogen, respectively. For mixed dimers AB, the following combination rule[22] was used

$$\rho_{AB} = 2\frac{\rho_A\rho_B}{\rho_A + \rho_B} \tag{4}$$

The ionization potentials of the atoms are given in Table 2, and the derived damping parameters of the dimers are given in Table 3. From these, the damped dispersion interaction energy at an intermonomer separation R was obtained as

$$dD = -f(\rho R)\sum_{n=6,8,10,\ldots} g_n(\rho R)\frac{C_n}{R^n} \tag{5}$$

$$f(x) = 1 - x^{1.68}\ \exp(-0.78x) \qquad (x = \rho R)$$

$$g_n(x) = [1 - \exp(-2.1x/n - 0.109x^2/n^{1/2})]^n$$

We note that the Tang-Toennies[62] damping functions gave similar results but require a fit to the repulsive part of the potential in order to extract the damping parameter.

2.5. Dispersion Coefficients. The long-range van der Waals dispersion coefficients C_n used are given in Table 3. We have tried to use the most accurate coefficients available in the literature. If they were not available, we have calculated them using a high level of theory and large basis sets with the POLCOR package,[30,31] extended[35,38] to use a DFT/Coupled Kohn−Sham (CKS) description of the monomer properties (thus allowing a good treatment of the intramonomer correlation). In a few cases, particularly for the open-shell compounds, the coefficients have been estimated using established rules. The details are given in the footnotes to Table 3.

3. Results and Discussion

We have tested the HFD and DFdD methods with different xc functionals for some simple dimers: three rare gas-rare gas complexes, Rg_2 (singlets: Ar_2, Kr_2, and Xe_2); five metal-rare gas complexes, M-Rg (singlets: Mg−He and Ca−Xe; doublets: Na−Ar, Cu−Ar, and Cu−Xe); and two metal−metal complexes, M_2 (singlet: Mg_2; triplet: Na_2). Some preliminary calculations were also performed for He_2 and H_2 triplet. The goals were to test the performance of the HFD method for these three classes of van der Waals complexes and determine if a DFdD method could be found that would perform equally well for all the classes. Thus, calculations were performed with various xc functionals.

3.1. DFT versus HF Interaction and Total Energies of Sample Complexes. From the work of Wu et al.[13] and our preliminary calculations, it was seen that the HFD method generally performs well. Thus, our goal became to find an xc functional that would reproduce the HF interaction energy. Since the HF and DFT interaction energies both rely on subtraction, we examined both the interaction energies and the total energies of dimers and monomers for a representative subset of the complexes and compared these to their HF counterparts. Table 4 shows this for two complexes from each of the three classes [Rg_2: Ar_2 and Xe_2; M-Rg: Ca−Xe and Cu−Xe (doublet); and M_2 complexes: Mg_2 and Na_2 (triplet)]. The calculations in the table were performed at near the correct minimum geometries of the complexes. The results shown correspond to the following functionals: LDAx and LDA; PBEx, PBEx+VWNc, and PBE; revPBEx, revPBEx+VWNc, and revPBE; RPBEx, RPBEx+VWNc, and RPBE; PBE0; and TPSSx, TPSSx+VWNc, and TPSS. The comparison is made with respect to the HF interaction and total energies.

The observations to be drawn from Table 4 are as follows. First let us examine only the total energies. Let DFTx be defined as the use of an exchange-only or an exchange plus local correlation-only functional, whereas standard DFT will refer to LDA, PBE, revPBE, RPBE, PBE0, and TPSS. We see that using a DFTx method without any correlation brings the total energies of all dimers and monomers closer to the HF values, as compared to the corresponding DFTx method which includes the local correlation (while the corresponding standard DFT has a performance that is usually about halfway between these two extremes). This is true for all of the DFTx methods except for the LDAx (Slater exchange) functional where sometimes LDA performs better than LDAx. Clearly, GGA exchange improves the energies over the local exchange functional. Next, we see that revPBEx often improves the energies over PBEx. This is not surprising since revPBE[44] was developed from PBE by tuning a parameter in the PBEx enhancement factor (and thereby relaxing the local Lieb-Oxford bound,[63] which in any case is a sufficient but not necessary component of DFT, the authors of ref 44 note that the integrated bound was always obeyed), in order to better reproduce with revPBE the experimental atomization energies of some molecules and also the experimental total energies of the molecules and their constituent atoms. RPBEx performs similarly for the total energies to revPBEx. Again, this is expected since RPBE[45] was designed to reproduce revPBE at small s (but without relaxing the local Lieb-Oxford bound).[63] However, note that Cu−Xe is an exception in that the total energies are given better by PBEx than by the two revised exchange functionals. The meta-GGA TPSSx does about as well (and sometimes better) than the revised exchange functionals (except for Na_2, where TPSSx+VWNc performs decently, but worse than the revised exchange functionals).

Now let us consider interaction energies, as compared to the HF values. Since the majority of the interaction energies obtained using the standard DFT xc functionals have large percentage errors (perhaps accidental exceptions are Ar_2 and Xe_2 with revPBE), they will not be discussed further and we

will consider only the DFTx values. For all metal-containing dimers, the revPBEx functionals perform well, as does the RPBEx and TPSSx exchange functionals for Cu−Xe. In fact, good reproduction of total energies correlates with good reproduction of interaction energies for the metal-containing complexes (except for the case of Na_2, with the TPSSx+VWNc exchange functional). This direct correspondence is missing in the case of the Rg_2 complexes. Here, instead, the revPBEx+VWNc functional performs best for interaction energies while revPBEx performed well for the total energies. (There appears to be a direct correspondence between good performance for total and interaction energies with the RPBEx and TPSSx functionals but our later work shows that they do not work as well as they could, particularly for the binding energy of Cu−Xe, see Table 5b.) Thus, due to the discrepancy with the total energies, unlike for the good performance of revPBEx for the interaction energies of metal-containing complexes, the apparent good performance of revPBEx+VWNc for the Rg_2 complexes is likely to be accidental.

3.2. Repulsive and Total Interaction Potentials of Complexes. Figures 2−4 show potential curves for the six sample complexes discussed above. Since the revPBEx+VWNc and revPBEx methods performed reasonably for the repulsive interaction energies of Rg_2 and metal-containing complexes, respectively, to avoid clutter we display potentials obtained with these two DFTx methods only. In each figure, the upper panels show the repulsive potentials (in a log-linear plot) compared to the HF potential, while the lower panels show the full potentials including the damped dispersion expansion compared to the HFD potential and benchmarks (CCSD(T), and if available literature ab initio and empirical benchmarks; note that the true benchmark for the Mg_2 potential is the ab initio literature calculation which includes FCI corrections). Examining the repulsive potentials, it is clear that all methods perform equally well at very close range (at least on a logarithmic scale). As the intermonomer separation R increases, a change in slope occurs which reflects the shell structures of the atoms comprising the dimer. At still larger R, the interaction energies given by the DFTx methods generally become too small and eventually become negative (even without any correlation; this is due to the self-interaction error present in DFT, which can mimic the effect of correlation), as compared to the "exact exchange" given by the HF curve. Examining these curves, it appears that one can predict a better repulsive interaction energy in the region of the attractive well (the usual region of interest) by extrapolating a DFTx repulsive curve from about the point where the slope of the curve changes toward the region of the minimum by fitting the points $E_{\mathrm{int,rep}}^{\mathrm{DFTx}}$ in the region $[R_1,R_2]$ with the form

$$\ln E_{\mathrm{int,rep,ext}}^{\mathrm{DFTx}} = \ln A^{\mathrm{DFTx}} - B^{\mathrm{DFTx}} R \qquad (6)$$

The fitting region $[R_1,R_2]$ was chosen for each system in such a way as to decently predict the region of the well (in comparison to HF and the benchmark full potentials, when the damped dispersion was added). This is the meaning of the extrapolated potentials marked "ext" in the figures and also in Table 5. In many cases, this procedure gave an improvement over the raw DFTx energies in comparison to HF and the DFdD energies in comparison to the benchmarks. The details, including the regions $[R_1,R_2]$ used for each complex, are given in the footnotes of Table 5. (Note that, if a double exponential form is chosen as in ref 22, the fitting region can be extended and perhaps the final result improved. However, a double exponential fit, although more appropriate for metal-containing complexes, cannot be linearized and thus the fitting will require more points and generally be more cumbersome. For this reason of economy we have chosen to use the single exponential form over a more limited range.)

Let us examine the full potentials (bottom portions) in these figures in detail. As observed above, the DFTx method with revPBEx+VWNc performs well for the Rg_2 complexes (however, based on the behavior of total energies, this good performance may be accidental) and the corresponding DFdD potential is reasonable. At the same time, the potential obtained without any correlation, revPBEx, is much too shallow. For the metal-containing complexes, the situation is the exact opposite: the DFdD method with revPBEx performs dramatically better while adding the correlation yields a curve much too deep. The effect of extrapolation is generally modest, except in the cases of the M_2 complexes, where there is a significant improvement.

In order to quantify these conclusions and present results with a larger set of DFT xc functionals (i.e., both standard DFT and DFdD based on DFTx) for all the complexes considered in this work, we have performed harmonic fits to both the standard DFT and the DFdD potentials (for the latter, both raw and extrapolated) and extracted (a) the minimum separation distance R_e, (b) the binding energy D_e, and (c) the harmonic frequency ω_e. For completeness, this was also done for the HFD and the MP2 and the CCSD(T) potentials. The results are presented in Table 5a−c, respectively.

In Table 5a−c, let us first consider the performance of the standard DFT xc functionals with respect to position of the minimum and the binding energy. For all complexes, LDA shifts the minimum to a shorter separation and vastly overbinds. In fact, the exchange part of LDA (the Slater exchange) is responsible for a majority of this attraction. Thus, use of LDA for weakly bound systems is not justified since the binding is of an unphysical origin (exchange rather than correlation) and thus any rough agreement of LDA results with more accurate calculations must be the result of error cancelations. The PBE and revised PBE xc functionals generally shift the minimum outward from the correct position and underbind (for Cu−Xe, PBE shifts it inward and overbinds). The hybrid PBE0 and the meta-GGA TPSS perform similarly to the revised PBE xc functionals. As for the frequencies, overbinding leads to a too-stiff curve and a too-large frequency while underbinding has the opposite effect.

Now let us examine the performance of the DFdD methods. Based on percentage differences and on the root-mean-square deviation (rmsd) summarizing the data, the only methods that seem to perform well across the board are the same ones noted before: DFdD with revPBEx+VWNc for the Rg_2 complexes and DFdD with revPBEx for the metal-containing complexes. Extrapolation does improve the results, sometimes modestly, but sometimes dramatically as for the D_e of Mg_2. The final performance of the best DFdD method for each complex (with extrapolation) is about as good as with HFD or MP2.

4. Conclusions

In their application to weakly bound complexes, modern DFT xc functionals exhibit two glaring deficiencies: lack of correct long-range attraction or correlation (also called dispersion) and incorrect repulsion (also called exchange). A troubling feature is that one error may mask the other (for example, exchange should always be repulsive for the types of complexes studied here but its incorrect representation in DFT may result in an unphysical attraction). In standard LDA, GGA, hybrid, or meta-GGA DFT, there is no inexpensive technique to self-consistently and correctly include the long-range correlation. It should be

possible to improve the exchange, however, and by testing different functionals in comparison to "exact exchange" as given by HF, we have tried to find one functional that would perform well for all the tested classes of complexes, the Rg_2, M−Rg, and M_2 representative dimers. This was done by adding an accurate damped dispersion contribution based on precalculated dispersion coefficients to the exchange contribution (sometimes also including the local correlation) obtained using various DFTx functionals. The DFdD potentials thus obtained were then compared to accurate benchmarks. We have found that no single DFTx functional performs ideally in all cases. However, the DFdD method with revPBEx+VWNc appears to work well for all metal-free dimers. Given the behavior of total energies, this apparent good performance may be accidental. For dimers containing metals, a better prescription is to avoid use of the local correlation altogether in the xc functional and thus instead use revPBEx. Extrapolation from shorter range of the repulsive potential alone with a simple exponential form improves the results in comparison to accurate benchmarks. The final results are comparable to HFD or MP2 at a fraction of the cost of the latter. Since even HF is extremely expensive in the plane-wave based codes generally used in calculations of physisorption on metal surfaces, developing a workable DFT-based method which can reasonably and physically model weak interactions should be a useful advance. The physisorption calculations using the methods developed and tested in this work will be presented in a subsequent paper. In addition, we hope that some of our observations may be useful in improving the performance of exchange functionals for weakly interacting systems.

Acknowledgment. G.M. thanks Christof Wöll and Volker Staemmler of the Ruhr-Universität Bochum for helpful discussions and acknowledges computer resources provided by CNR-INFM DEMOCRITOS and CINECA. G.M. thanks R. Podeszwa for supplying the code for the CKS-based POLCOR and for assistance in its use.

References and Notes

(1) Brivio, G. P.; Trioni, M. I. *Rev. Mod. Phys.* **1999**, *71*, 231.
(2) Hohenberg, P.; Kohn, W. *Phys. Rev.* **1964**, *136*, B864.
(3) Kohn, W.; Sham, L. *J. Phys. Rev.* **1965**, *140*, A1133.
(4) Greeley, J.; Nørskov, J. K.; Mavrikakis, M. *Annu. Rev. Phys. Chem.* **2002**, *53*, 319.
(5) Fratesi, G.; de Gironcoli, S. *J. Chem. Phys.* **2006**, *125*, 044701.
(6) Mazzarello, R.; Cossaro, A.; Verdini, A.; Rousseau, R.; Casalis, L.; Danisman, M. F.; Floreano, L.; Scandolo, S.; Morgante, A.; Scoles, G. *Phys. Rev. Lett.* **2007**, *98*, 016102.
(7) Philipsen, P. H. T.; Baerends, E. J. *Phys. Rev. B* **1996**, *54*, 5326.
(8) Bruch, L. W.; Cole, M. W.; Zaremba, E. *Physical adsorption: Forces and phenomena*; Oxford: New York, 1997.
(9) Diehl, R. D.; Seyller, T.; Caragiu, M.; Leatherman, G. S.; Ferralis, N.; Pussi, K.; Kaukasoina, P.; Lindroos, M. *J. Phys.: Condens. Matter* **2004**, *16*, S2839.
(10) Bruch, L. W.; Diehl, R. D.; Venables, J. A. *Rev. Mod. Phys.* **2007**, *79*, 1381.
(11) Perdew, J. P.; Ruzsinszky, A.; Tao, J.; Staroverov, V. N.; Scuseria, G. E.; Csonka, G. I. *J. Chem. Phys.* **2005**, *123*, 062201.
(12) Tao, J. M.; Perdew, J. P.; Staroverov, V. N.; Scuseria, G. E. *Phys. Rev. Lett.* **2003**, *91*, 146401.
(13) Wu, X.; Vargas, M. C.; Nayak, S.; Lotrich, V.; Scoles, G. *J. Chem. Phys.* **2001**, *115*, 8748.
(14) Tsuzuki, S.; Lüthi, H. P. *J. Chem. Phys.* **2001**, *114*, 3949.
(15) Sharma, M.; Resta, R.; Car, R. *Phys. Rev. Lett.* **2007**, *98*, 247401.
(16) Marini, A.; García-González, P.; Rubio, A. *Phys. Rev. Lett.* **2006**, *96*, 136404.
(17) Dion, M.; Rydberg, H.; Schröder, E.; Langreth, D. C.; Lundqvist, B. I. *Phys. Rev. Lett.* **2004**, *92*, 246401.
(18) Dion, M.; Rydberg, H.; Schröder, E.; Langreth, D. C.; Lundqvist, B. I. *Phys. Rev. Lett.* **2005**, *95*, 109902(E)
(19) Thonhauser, T.; Cooper, V. R.; Li, S.; Puzder, A.; Hyldgaard, P.; Langreth, D. C. *Phys. Rev. B* **2007**, *76*, 125112.
(20) Podeszwa, R.; Szalewicz, K. *Chem. Phys. Lett.* **2005**, *412*, 412.
(21) Polo, V.; Gräfenstein, J.; Kraka, E.; Cremer, D. *Chem. Phys. Lett.* **2002**, *352*, 469.
(22) Douketis, C.; Scoles, G.; Marchetti, S.; Zen, M.; Thakkar, A. J. *J. Chem. Phys.* **1982**, *76*, 3057.
(23) Jeziorski, B.; Moszynski, R.; Szalewicz, K. *Chem. Rev.* **1994**, *94*, 1887.
(24) Jeziorski, B.; Szalewicz, K. *Symmetry-adapted perturbation theory. In Handbook of Molecular Physics and Quantum Chemistry*; Wilson, S., Ed.; Wiley: New York, 2003; Vol. 3, p 232.
(25) Boys, S. F.; Bernardi, F. *Mol. Phys.* **1970**, *19*, 553.
(26) Chałasiński, G.; Szczęśniak, M. M. *Chem. Rev.* **1994**, *94*, 1723.
(27) Raghavachari, K.; Trucks, G. W.; Pople, J. A.; Head-Gordon, M. *Chem. Phys. Lett.* **1989**, *157*, 479.
(28) Patkowski, K.; Murdachaew, G.; Fou, C. M.; Szalewicz, K. *Mol. Phys.* **2005**, *103*, 2031.
(29) Bukowski, R.; Szalewicz, K.; Groenenboom, G. C.; van der Avoird, A. *Science* **2007**, *315*, 1249.
(30) Wormer, P. E. S.; Hettema, H. *J. Chem. Phys.* **1992**, *97*, 5592.
(31) Wormer, P. E. S.; Hettema, H. *POLCOR package*; University of Nijmegen: Nijmegen, The Netherlands, 1992.
(32) Misquitta, A. J.; Szalewicz, K. *Chem. Phys. Lett.* **2002**, *357*, 301.
(33) Misquitta, A. J.; Jeziorski, B.; Szalewicz, K. *Phys. Rev. Lett.* **2003**, *91*, 033201.
(34) Misquitta, A. J.; Szalewicz, K. *J. Chem. Phys.* **2005**, *122*, 214109.
(35) Misquitta, A. J.; Podeszwa, R.; Jeziorski, B.; Szalewicz, K. *J. Chem. Phys.* **2005**, *123*, 214103.
(36) Bukowski, R.; Cencek, W.; Jankowski, P.; Jeziorska, M.; Jeziorski, B.; Kucharski, S. A.; Lotrich, V. F.; Misquitta, A. J.; Moszyński, R.; Patkowski, K.; Podeszwa, R.; Rybak, S.; Szalewicz, K.; Williams, H. L.; Wheatley, R. J.; Wormer, P. E. S.; Zuchowski, P. S. *SAPT2006.2: An Ab initio Program for Many-Body Symmetry-Adapted Perturbation Theory Calculations of Intermolecular Interaction Energies*; University of Delaware and University of Warsaw: Newark, DE, 2006; http://www.physics.udel.edu/szalewic/SAPT/SAPT.html.
(37) Podeszwa, R.; Bukowski, R.; Szalewicz, K. *J. Phys. Chem. A* **2006**, *110*, 10345.
(38) Patkowski, K.; Podeszwa, R.; Szalewicz, K. *J. Phys. Chem. A* **2007**, *111*, 12822.
(39) Examples of recent advances include Kohn-Sham rather than Hartree-Fock description of monomers within SAPT(DFT), use of density fitting within HF, DFT, MP2, and SAPT(DFT), and so-called local approaches potentially allowing linear scaling.
(40) Bukowski, R.; Podeszwa, R.; Szalewicz, K. *Chem. Phys. Lett.* **2005**, *414*, 111.
(41) Slater, J. C. *Phys. Rev.* **1951**, *81*, 385.
(42) Vosko, S. H.; Wilk, L.; Nusair, M. *Can. J. Phys.* **1980**, *58*, 1200 (We used VWN5, the version implemented in most computational chemistry packages).
(43) Perdew, J. P.; Burke, K.; Ernzerhof, M. *Phys. Rev. Lett.* **1996**, *77*, 3865.
(44) Zhang, Y.; Yang, W. *Phys. Rev. Lett.* **1998**, *80*, 890.
(45) Hammer, B.; Hansen, L. B.; Nørskov, J. K. *Phys. Rev. B* **1999**, *59*, 7413.
(46) Adamo, C.; Barone, V. *J. Chem. Phys.* **1999**, *110*, 6158.
(47) Zhang, Y.; Pan, W.; Yang, W. *J. Chem. Phys.* **1997**, *107*, 7921.
(48) Lacks, D. J.; Gordon, R. G. *Phys. Rev. A* **1993**, *47*, 4681.
(49) Werner, H.-J.; Knowles, P. J.; Lindh, R.; Manby, F. R.; Schütz, M.; Celani, P.; Korona, T.; Rauhut, G.; Amos, R. D.; Bernhardsson, A.; Berning, A.; Cooper, D. L.; Deegan, M. J. O.; Dobbyn, A. J.; Eckert, F.; Hampel, C.; Hetzer, G.; Lloyd, A. W.; McNicholas, S. J.; Meyer, W.; Mura, M. E.; Nicklass, A.; Palmieri, P.; Pitzer, R.; Schumann, U.; Stoll, H.; Stone, A. J.; Tarroni, R.; Thorsteinsson, T. MOLPRO, a package of ab initio programs, versions, 2002.6 and 2006.1; 2002, 2006; http://www.molpro.net.
(50) Bylaska, E. J.; de Jong, W. A.; Kowalski, K.; Straatsma, T. P.; Valiev, M.; Wang, D.; Aprà, E.; Windus, T. L.; Hirata, S.; Hackler, M. T.; Zhao, Y.; Fan, P.-D.; Harrison, R. J.; Dupuis, M.; Smith, D. M. A.; Nieplocha, J.; Tipparaju, V.; Krishnan, M.; Auer, A. A.; Nooijen, M.; Brown, E.; Cisneros, G.; Fann, G. I.; Früchtl, H.; Garza, J.; Hirao, K.; Kendall, R.; Nichols, J. A.; Tsemekhman, K.; Wolinski, K.; Anchell, J.; Bernholdt, D.; Borowski, P.; Clark, T.; Clerc, D.; Dachsel, H.; Deegan, M.; Dyall, K.; Elwood, D.; Glendening, E.; Gutowski, M.; Hess, A.; Jaffe, J.; Johnson, B.; Ju, J.; Kobayashi, R.; Kutteh, R.; Lin, Z.; Littlefield, R.; Long, X.; Meng, B.; Nakajima, T.; Niu, S.; Pollack, L.; Rosing, M.; Sandrone, G.; Stave, M.; Taylor, H.; Thomas, G.; van Lenthe, J.; Wong, A.; Zhang, Z. *NWChem, A Computational Chemistry Package for Parallel Computers, version 5.0*; Pacific Northwest National Laboratory: Richland, WA 99352−0999, USA, 2006; http://www.emsl.pnl.gov/docs/nwchem/nwchem.html.
(51) Frisch, M. J.; Trucks, G. W.; Schlegel, H. B.; Scuseria, G. E.; Robb, M. A.; Cheeseman, J. R.; Montgomery, Jr., J. A.; Vreven, T.; Kudin, K. N.; Burant, J. C.; Millam, J. M.; Iyengar, S. S.; Tomasi, J.; Barone, V.; Mennucci, B.; Cossi, M.; Scalmani, G.; Rega, N.; Petersson, G. A.; Nakatsuji, H.; Hada, M.; Ehara, M.; Toyota, K.; Fukuda, R.; Hasegawa, J.;

Ishida, M.; Nakajima, T.; Honda, Y.; Kitao, O.; Nakai, H.; Klene, M.; Li, X.; Knox, J. E.; Hratchian, H. P.; Cross, J. B.; Bakken, V.; Adamo, C.; Jaramillo, J.; Gomperts, R.; Stratmann, R. E.; Yazyev, O.; Austin, A. J.; Cammi, R.; Pomelli, C.; Ochterski, J. W.; Ayala, P. Y.; Morokuma, K.; Voth, G. A.; Salvador, P.; Dannenberg, J. J.; Zakrzewski, V. G.; Dapprich, S.; Daniels, A. D.; Strain, M. C.; Farkas, O.; Malick, D. K.; Rabuck, A. D.; Raghavachari, K.; Foresman, J. B.; Ortiz, J. V.; Cui, Q.; Baboul, A. G.; Clifford, S.; Cioslowski, J.; Stefanov, B. B.; Liu, G.; Liashenko, A.; Piskorz, P.; Komaromi, I.; Martin, R. L.; Fox, D. J.; Keith, T.; Al-Laham, M. A.; Peng, C. Y.; Nanayakkara, A.; Challacombe, M.; Gill, P. M. W.; Johnson, B.; Chen, W.; Wong, M. W.; Gonzalez, C.; Pople, J. A. *Gaussian 03, revision D.02*; Gaussian, Inc.: Wallingford, CT, 2004.

(52) Knowles, P. J.; Hampel, C.; Werner, H.-J. *J. Chem. Phys.* **1993**, *99*, 5219.

(53) Knowles, P. J. *J. Chem. Phys.* **2000**, *112*, 3106.

(54) Tao, F.-M.; Pan, Y.-K. *J. Chem. Phys.* **1992**, *97*, 4989.

(55) Williams, H. L.; Mas, E.; Szalewicz, K.; Jeziorski, B. *J. Chem. Phys.* **1995**, *103*, 7374.

(56) Bergner, A.; Dolg, M.; Kuechle, W.; Stoll, H.; Preuss, H. *Mol. Phys.* **1993**, *80*, 1431.

(57) Figgen, D.; Rauhut, G.; Dolg, M.; Stoll, H. *Chem. Phys.* **2005**, *311*, 227.

(58) Martin, J. M. L.; Sundermann, A. *J. Chem. Phys.* **2001**, *114*, 3408.

(59) Peterson, K. A.; Figgen, D.; Goll, E.; Stoll, H.; Dolg, M. *J. Chem. Phys.* **2003**, *119*, 11113.

(60) Peterson, K. A.; Puzzarini, C. *Theor. Chem. Acc.* **2005**, *114*, 283.

(61) Patkowski, K.; Szalewicz, K. *J. Chem. Phys.* **2007**, *127*, 164103.

(62) Tang, K. T.; Toennies, J. P. *J. Chem. Phys.* **1984**, *80*, 3726.

(63) Lieb, E. H.; Oxford, S. *Int. J. Quantum Chem.* **1981**, *19*, 427.

(64) EMSL Basis Set Exchange Library, http://gnode2.pnl.gov/bse/portal.

(65) Woon, D. E.; Dunning, T. H., Jr *J. Chem. Phys.* **1994**, *100*, 2975.

(66) Woon, D. E.; Dunning, T. H., Jr. to be published.

(67) Woon, D. E.; Dunning, T. H., Jr *J. Chem. Phys.* **1993**, *98*, 1358.

(68) Peterson, K. A.; Dunning, T. H., Jr *J. Chem. Phys.* **2002**, *117*, 10548.

(69) Koput, J.; Peterson, K. A. *J. Phys. Chem. A* **2002**, *106*, 9595.

(70) Schmidt, M. W.; Ruedenberg, K. *J. Chem. Phys.* **1979**, *71*, 3951.

(71) Lias, S. G. *Ionization Energy Evaluation. In NIST Chemistry WebBook, NIST Standard Reference Database Number 69*; Linstrom, P. J., Mallard, W. G., Eds.; National Institute of Standards and Technology: Gaithersburg, MD, 2005; http://webbook.nist.gov.

(72) Kislyakov, I. M. *Opt. Spectrosc.* **1999**, *87*, 357.

(73) Hattig, C.; Hess, B. A. *J. Phys. Chem.* **1996**, *100*, 6243.

(74) Thakkar, J. *J. Chem. Phys.* **1988**, *89*, 2092.

(75) Proctor, T. R.; Stwalley, W. C. *J. Chem. Phys.* **1977**, *66*, 2063.

(76) Chu, X.; Dalgarno, A. *J. Chem. Phys.* **2004**, *121*, 4083.

(77) Derevianko, A.; Johnson, W. R.; Safronova, M. S.; Babb, J. F. *Phys. Rev. Lett.* **1999**, *82*, 3589.

(78) Porsev, S. G.; Derevianko, A. *J. Chem. Phys.* **2003**, *119*, 844.

(79) Aziz, R. A. *J. Chem. Phys.* **1993**, *99*, 4518.

(80) Slavíček, P.; Kalus, R.; Paška, P.; Odvárková, I.; Hobza, P.; Malijevský, A. *J. Chem. Phys.* **2003**, *119*, 2102.

(81) Dham, A. K.; Allnatt, A. R.; Meath, W. J.; Aziz, R. A. *Mol. Phys.* **1989**, *67*, 1291.

(82) Dham, A. K.; Meath, W. J.; Allnatt, A. R.; Aziz, R. A.; Slaman, M. *J. Chem. Phys.* **1990**, *142*, 173.

(83) Hinde, R. J. J. *Phys. B: At. Mol. Opt. Phys.* **2003**, *36*, 3119.

(84) Czuchaj, E.; Krosnicki, M.; Stoll, H. *Chem. Phys.* **2003**, *292*, 101.

(85) Tellinghuisen, J.; Ragone, A.; Kim, M. S.; Auerbach, D. J.; Smalley, R. E.; Wharton, L.; Levy, D. H. *J. Chem. Phys.* **1979**, *71*, 1283.

(86) Shen, Y.; BelBruno, J. J. *J. Phys. Chem. A* **2005**, *109*, 10077.

(87) Tiesinga, E.; Kotochigova, S.; Julienne, P. S. *Phys. Rev. A* **2002**, *65*, 042722.

(88) Gutowski, M. *J. Chem. Phys.* **1999**, *110*, 4695.

JP800974K